An effective stress approach to modelling mine backfilling

M. Helinski, M. Fahey, The University of Western Australia, Perth, Western Australia, and
A.B. Fourie, Australian Centre for Geomechanics, The University of Western Australia,
Perth, Western Australia

ABSTRACT **This paper presents the results of a research project that is currently underway aimed at furthering the understanding of geotechnical aspects associated with the placement of tailings, based mine backfill. The aim of the work was to develop a model and experimental strategy capable of capturing all of the significant mechanisms associated with the minefill process. The model is based on fundamental material properties and is therefore capable of simulating the placement of all hydraulically placed fill types ranging from coarse hydraulic fills through to fine paste fill and any combination in between. Using this model to simulate different minefill materials, the authors have been able to gain an improved understanding of the interaction of various mechanisms associated with the filling process and provide an insight into problematic minefill aspects such as barricade loads and the application of effective stress *in situ*. It has been shown that the consolidation of mine backfill has a major impact on barricade loads and that material properties that may appear subtle can actually have a significant influence on the consolidation process and therefore barricade loads.**

KEYWORDS Backfill, Effective stress, Model, Coupled analysis

INTRODUCTION

Tailings-based mine backfilling is the process whereby tailings are combined with small amounts of cement (generally 0% to 10%) and water before being used to fill previously mined voids in an open stope mining operation. In order to contain the material in a stope (stopping it from flowing into nearby mine workings), containment barricades are constructed in the stope drawpoint. Design of these barricades appears to be problematic; the authors are aware of eight barricade failures in 2003 and of a further five failures in the past year.

As demonstrated by Helinski, Fourie, & Fahey (2006), the extent to which consolidation occurs and effective stress develops in the backfill during placement has a major effect on barricade loads. In an effort to gain an improved understanding of the filling process and hence of the loads that are placed on these containment structures, the authors have developed a fully coupled plane strain and axisymmetric numerical model, called "Minefill-2D." This model simulates the filling process, taking account of all of the significant mechanisms. It is believed that this type of tool is required to provide a rigorous technique for estimating barricade loads in both paste and hydraulic fills. The model can also be used to assess the influence of subtle changes in material properties and filling sequences on these loads.

A number of authors have demonstrated that for the same mix, *in situ* material strengths can be far greater than those measured in the laboratory (Le Roux, Bawden, & Grabinski, 2002; Revell 2004). Therefore, another application for this tool will be to develop an understanding of the processes involved during curing of material *in situ*. This type of tool can provide information about the rate that effective stress is being applied to the samples as it is cured *in situ* and the transfer of water within the fill mass for different fill types. With an improved understanding of how minefill material is cured *in situ,* laboratory curing methods can be tailored to more suitably represent field curing conditions.

In this paper, Minefill-2D is used to investigate the influence of different tailings properties on the behaviour during placement. Focus is placed on the interaction of the different mechanisms and how these impact on calculated barricade stresses.

COMPUTER PROGRAM "MINEFILL-2D"

Simulation of minefill drainage has been previously addressed by authors such as Isaacs and Carter (1993) and Traves and Isaacs (1991), while the simulation of stress development during filling (neglecting the influence of pore pressures) has been undertaken by Rankine, Rankine, Sivakugan, Karunasena, & Bloss (2001) and Belem, El Aatar, Bussiere, Benzaazoua, Fall, & M. Yilmaz (2006). To the authors' knowledge, Minefill-2D is the first model that attempts to couple pore pressures and stress development, as well as all of the other significant mechanisms associated with

filling a stope with cemented tailings-based backfill. While the current version of the model is only two-dimensional (plane strain or axisymmetric), the authors believe that in many cases it can appropriately be used to estimate barricade loads.

The model is a finite element fully coupled consolidation model that is based on the consolidation theory of Biot (1941). It also takes account of the following:

- Stiffness—Aspects that can influence the material stiffness include the initial uncemented density, cement hydration, and damage to the cement bonds due to excessive strain.
- Strength—This can be influenced by cement hydration as well as destruction of cement bonds due to excessive stress or strain.
- Hydraulic conductivity—This can be influenced by material density, particle size distribution, and cement hydration.
- Self desiccation—This refers to the net water volume change that occurs as a result of the chemical reactions associated with the hydration process (Helinski, Fourie, & Fahey, 2007).

Other characteristics of the model incorporated into Minefill-2D include:

- Progressive rising of the fill surface (at any given rate) during the consolidation / hydration process to represent the accretion of material within the stope.
- The Mohr-Coulomb yield criterion has been adopted to represent the material strength. This allows for internal yielding, and also for yielding at the interface between the fill mass and the surrounding rockmass.
- A non-linear stiffness model has been adopted such that the small strain (or initial tangent) stiffness is used initially, but this stiffness reduces as the stress approaches the yield stress in accordance with the non-linear stiffness function suggested by Fahey and Carter (1993).
- A strain-softening model has been used such that the cementation is progressively destroyed as the material is strained beyond yield.
- The water table is allowed to rise and fall according to volumetric strains and flows through the upper material layer. The elevation of the water table dictates the pore pressures at the surface nodes.
- Calculations are performed in terms of total water head rather than excess pore pressure.
- The current version of the model assumes fully saturated conditions throughout the filling process.

LABORATORY TESTWORK

The testing procedure devised to provide input parameters to the model involves a minimum of two tests. These include a "hydration test" and a consolidated drained triaxial test.

The hydration test is used to measure the properties relating to stiffness development, hydraulic conductivity, and self desiccation. It involves preparing a sample in a cell as illustrated in Figure 1. A triaxial membrane is stretched inside a perforated mould and secured to the sample base pedestal of the apparatus. The tailings material, in a slurry form, is poured into the membrane, which is then sealed to the top cap, just as in standard triaxial testing practice. However, in this case, the perforated mould is left in place for the duration of the hydration test.

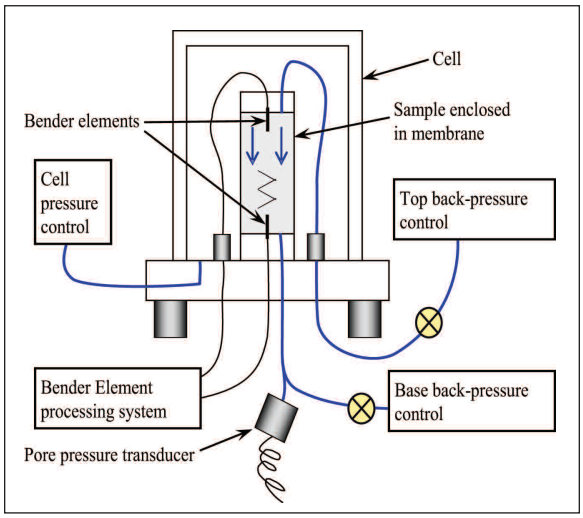

Fig. 1. Hydration test setup.

The cell pressure and back pressure are then ramped up simultaneously to the final target values, maintaining a constant difference between them in this process. After allowing some time for saturation, the back-pressure valves are then closed and the cell pressure is ramped up to the desired level. During this phase, Skempton's *B* value can be assessed to confirm saturation.

Once an appropriate cell pressure is reached, a hydraulic gradient is applied across the sample to measure the hydraulic conductivity. This can be carried out at any stage during the hydration period to assess the change in hydraulic conductivity due to the formation of the cement gel within the voids. In order to represent the dependence of the hydraulic conductivity of the material on the void ratio, the function suggested by Carrier, Bromwell, & Somogyi (1983) has been adopted:

$$k = \frac{c_k (e_{ff})^{d_k}}{1+e} \qquad (1)$$

where e is the actual void ratio, c_k and d_k are constants, and e_{ff} is the effective void ratio that is determined from the initial void ratio and the increase in

volume of solids due to the growth of the cement product and any compression of the soil matrix. The cement product volume is inclusive of both the cement solids and gel, as the gel is considered to have a hydraulic conductivity that is infinitely low relative to the tailings.

Bender elements (Dyvik & Olsen, 1989; Baig, Picornell, & Nazarian, 1997; Fernandez & Santamarina, 2001) are attached to the sample end platens. The bender element at the top of the sample is used to generate shear waves, which travel through the sample at shear wave velocity V_s, and are detected by the receiver element at the opposite end of the sample. Since shear wave velocity depends only on the initial tangent (or small strain) shear stiffness G_{max} and the bulk density of the material (ρ), a value of G_{max} can be obtained from these tests (Dyvik & Olsen, 1989):

$$G_{max} = \rho(V_s)^2 \qquad (2)$$

Thus, the change in G_{max} can be measured non-destructively with this equipment throughout the hydration process. This change in G_{max} with ongoing hydration has been shown to be representative of the development of other cementation-related properties such as the reduction in hydraulic conductivity and strength gain (Helinski et al., 2007). The material stiffness is assumed to develop with time t after the time t_o required for initial set, in accordance with the exponential function suggested by Rastrup (1956):

$$G_{max} = G_{max-i} + \Delta G_{max-f} .\exp\left(\frac{-d}{\sqrt{t}}\right) \qquad (3)$$

where G_{max} is the small strain shear stiffness at any time t after initial set, G_{max-i} is the initial (uncemented) value, ΔG_{max-f} is the ultimate increase that occurs during the whole hydration process, and d is a maturity term that dictates the rate of stiffness development. The small-strain bulk stiffness K_{max} can be obtained from G_{max} using elastic solutions (with an assumed value of the small strain Poisson's ratio). Thus, K_{max} increases from an initial value of K_{max-I} to a final value of K_{max-f} at the end of hydration. Similar functions represent the hydration-induced changes in other material properties.

Between hydraulic conductivity tests, the valves connected to the back pressure cells can be closed and the pore pressure monitored. Due to the self desiccation process that occurs during the hydration reaction (Helinski et al., 2007), the pore pressure generally reduces. Given the material stiffness and the drop in pore pressure, the water consumed in hydration can be determined with time. Combining the function suggested by Helinski et al. (2007) for total volumetric change, with the exponential term suggested by Rastrup (1956) to represent the progress of hydration, a function can be obtained to represent the cumulative volumetric change (V_w) with time. This function may be differentiated to represent the rate of volumetric change during hydration:

$$\frac{\delta(V_w/W_c)}{\delta t} = 0.5.E_h.\left(\frac{d}{t^{1.5}}\right).\exp\left(\frac{-d}{\sqrt{t}}\right) \qquad (4)$$

where W_c represents the mass of unhydrated cement, d represents the rate of hydration (in days$^{1/2}$; as determined from the rate of development of stiffness with time, equation 3), and E_h is the efficiency of hydration for the given tailings/binder combination (cm^3/g). The efficiency of hydration is a measure of the total volume change that occurs during the chemical reactions associated with cement hydration. It should be noted that different types of binder, tailings, or water can create different chemical reactions that have different volume changes.

Once the hydration process is complete, the sample is removed from the "hydration test" cell and placed in a normal triaxial testing apparatus in order to carry out a consolidated drained triaxial test. For the tests reported in this paper, a back pressure of 200 kPa and a cell pressure of 300 kPa were used (i.e. an initial effective confining pressure of 100 kPa). These samples were fitted with local strain gauges to measure the small strain response of the material. When sheared under a known stress path, the peak and residual material properties can be determined. A typical stress-strain plot from one of the triaxial tests is shown in Figure 2.

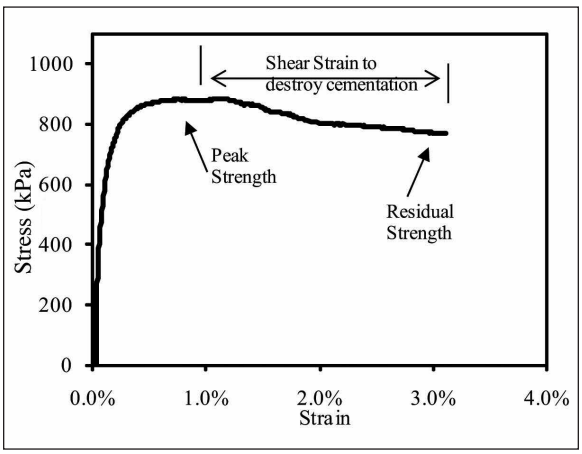

Fig. 2. Typical triaxial test result.

For this work, it has been assumed that the friction angles (ϕ′) for uncemented and cemented material are equal, and the difference in strength can be expressed using an effective cohesion component (c′)—in effect, the Mohr-Coulomb strength envelopes for uncemented and cemented material are parallel. From the results of the triaxial tests, the value of c′

and ϕ' at a given time during the hydration period can be determined. The evolution of c' is assumed to occur in a similar manner to the evolution of G_{max}, so that equation 3 can be re-cast to be in terms of c', and combined with the results of the shearing test to determine a relationship between c' and time throughout the hydration period. In addition to the strength parameters (c' and ϕ'), the triaxial test also provides a measure of the shear strains that are required to break down the cementation (as indicated in Figure 2). This characteristic is important in the strain softening model (incorporated in Minefill-2D) to represent the breakdown of cementation that may occur as a result of shearing at the fill-rock interface.

EXPERIMENTAL RESULTS

The main purpose of the testing program was to determine the impact of different tailings on the fundamental material properties. The properties that have been taken into consideration include the rate of cement hydration (d), the time until initial set (t_o), the efficiency of hydration (E_h), and the hydraulic conductivity parameters c_k and d_k (equation 1) for different materials of equal ultimate strengths. These material properties can then be used with Minefill-2D to assess the impact of the material properties on the interaction of mechanisms during placement, and in turn on the loads that would be placed on barricades.

The materials used in the study included a hydraulic fill (HF) material (Minefill A) obtained from the coarser cycloned fraction of a tailings stream, and two pastefill (PF) materials (Minefills B and C) obtained from full stream tailings. The particle size distribution (PSD) curves for these are presented in Figure 3. Each of the samples was prepared to a nominal void ratio of 0.9, with 3% by dry weight of added General Portland cement. The results of this testwork are summarized in Table 1.

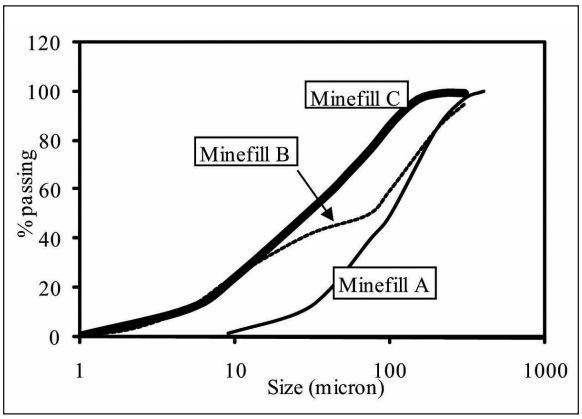

Fig. 3. Particle size distribution curves for tailings tested.

Table 1. Material properties

	Minefill A (HF)	Minefill B (PF)	Minefill C (PF)
$K_{max\text{-}i}$ (MPa)	80	50	31
$K_{max\text{-}f}$ (MPa)	630	750	950
d (day$^{1/2}$)	1.2	1.4	2.3
t_o (day)	0.2	0.2	0.2
E_h (cm^3/g)	0.064	0.032	0.018
c_k (m/s)	2.6 x 10^{-6}	5.0 x 10^{-6}	5.0 x 10^{-8}
d_k (-)	20	40	10
c'_{max} (kPa)	110	125	116
ϕ' (°)	35	30	28
$q_{u\text{-}f}$ (kPa)	422	433	380

From Table 1, it can be seen that the ultimate unconfined compressive strengths ($q_{u\text{-}f}$) are very similar for the three samples, even though the three materials have different values of d (the measure of the rate of stiffness/strength development), E_h (the efficiency of hydration), and c_k and d_k (the hydraulic conductivity parameters). Figures 4 and 5 show the evolution with time of hydraulic conductivity (k) and cohesion (c'), respectively.

MODELLING

In order to assess the impact of the various material properties on the filling process, Minefill-2D was used (in plane strain mode) to model the filling of a plane strain stope with width of 20 m and

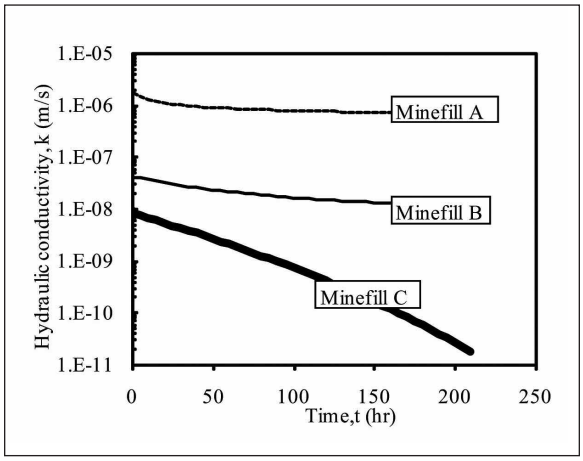

Fig. 4. Plot of the evolution of hydraulic conductivity against time for the different backfill types.

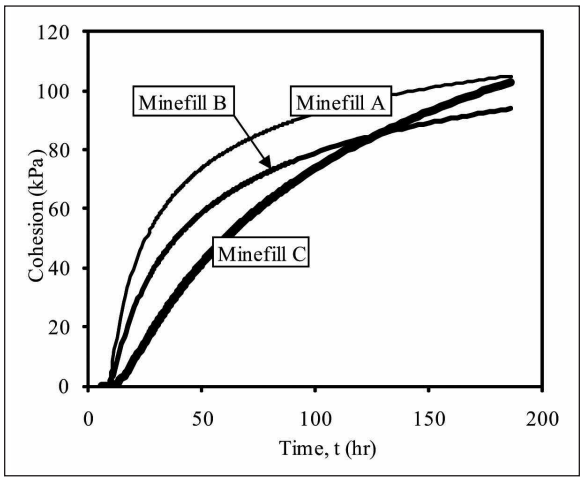

Fig. 5. Development of the c' component of strength against time for different backfill types.

height of 40 m. A drawpoint height of 5 m was adopted with a barricade offset distance of 5 m. A boundary condition of zero pore pressure was assigned along the boundary that represents the barricade. In order to allow direct comparison between the various materials, a standard filling sequence was adopted. This sequence consisted of filling the first 8 m over a 16-hour period (0.5 m/hr) followed by a 14-hour rest period, and then filling the remaining 42 m over a period of 84 hours (0.5 m/hr filling period).

In an actual stope, the drawpoint width is typically less than the side length of the stope, whereas in the plane strain representation it occupies the full side length. This means that the drawpoint represents a greater "choke" to outflow than the plane strain representation. In order to account for this, the hydraulic conductivity in the drawpoint area was halved for each case.

EFFECT OF VARIATIONS IN TAILINGS PROPERTIES

Modelling was undertaken using the material properties presented in Table 1 to assess the impact of tailings type on the resultant barricade loads.

Figure 6 shows a plot of the total horizontal stress developed at a point immediately behind the barricades for the various fill materials using the described filling sequence. This indicates that barricade stresses reach 108 kPa, 150 kPa, and 240 kPa for filling with Minefill B, Minefill A, and Minefill C, respectively. Thus, even with fills that reach the same ultimate strength ($q_{u\text{-}f}$), the loads that are placed on barricades can vary significantly.

It is interesting to note that there is no obvious relationship between any one material property and the resulting barricade loads. For example, barricade loads for Minefill B are the lowest, even though the hydraulic conductivity of Minefill A is higher while that of Minefill C is lower. Also, Minefill A shows a faster rate of hydration (lowest d value) and a higher efficiency of hydration (highest E_h value) compared to the other materials tested, but ranks in the middle in terms of ultimate barricade loads.

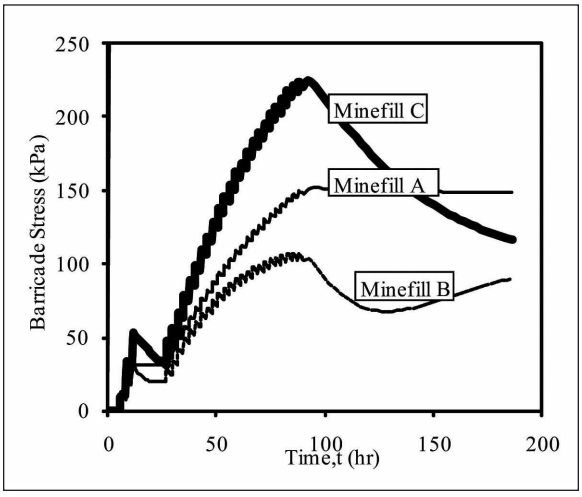

Fig. 6. Barricade load against time for different tailings.

The reasons for the load variation may be better understood by referring to the development of pore pressure within the stope. The development of pore pressure (against time) at the opposite side of the stope to the barricade is presented in Figure 7. Also shown in Figure 7 is the "steady state seepage pore pressure" that is created when the water table is maintained at the fill surface and zero pore pressure condition is maintained at the barricade boundary. This has been calculated in accordance with the relationship presented by Helinski and Grice (2007). Pore pressures greater than this value indicate that the material has not fully consolidated, while pore pressures equal to this value indicate that the material has completely consolidated. This is a somewhat artificial situation, since ongoing water flow without further addition of water to the stope would result in lowering of the water table (with the possibility of further consolidation as the equilibrium situation changes).

Comparison between Figures 6 and 7 indicates that there is a relationship between the development of pore pressure in a stope and barricade loads. This is logical, since higher pore pressures are associated with less consolidation and low effective stress.

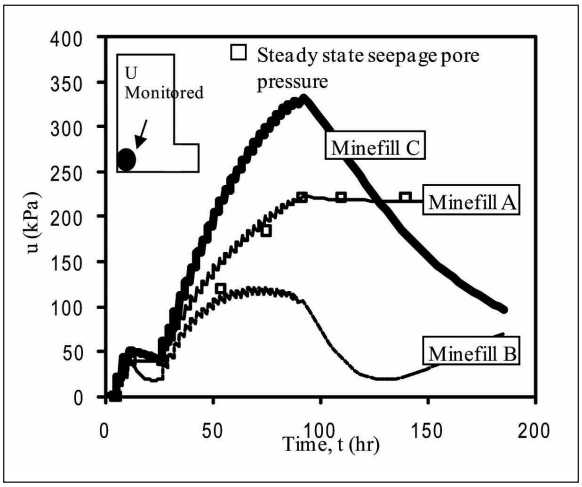

Fig. 7. Development of pore pressure against time.

As demonstrated by Helinski et al. (2006), with less effective stress, less interface shear strength is mobilized, resulting in higher total vertical stresses in the stope. In addition, the conversion of total vertical stress to total horizontal stress adjacent to the drawpoint is dependent both on the load being carried by the soil skeleton (effective stress) and that carried by the pore water (pore pressure), in accordance with equation 5:

$$\sigma_h = \sigma'_v.K_o + u \qquad (5)$$

where σ_h is the total horizontal stress, σ'_v is the vertical effective stress, K_o is the lateral earth pressure coefficient (≈ 0.3), and (*u*) is the pore pressure.

Therefore, if all of the total vertical stress is taken by the pore pressure (*u*), the vertical and horizontal total stresses will be equal, while if there is no pore pressure, the horizontal total stress will be approximately 30% of the total vertical stress.

The other aspect to note about Figure 7 is with respect to the development of pore pressure (for the different minefill materials) relative to the steady state seepage pore pressure. Comparing the pore pressures for the three cases with the steady state seepage pore pressure, it is clear that Minefill A exhibits steady state seepage pore pressures throughout the filling process, indicating immediate consolidation, Minefill C develops pore pressures that are greater than steady state seepage pore pressures indicating that consolidation is not complete, and Minefill B exhibits pore pressures that are even less than steady state seepage pore pressures. This may be more clearly understood through inspection of Figure 8, which shows the pore pressure isochrones along the stope centre line at the completion of filling. Also shown in Figure 8 is the line representing the steady state seepage pore pressures for the stope.

It is suggested that the reason for the three different types of behaviour is as follows.

MINEFILL A

Due to its high coefficient of consolidation (i.e. higher permeability, but stiffness comparable to the other two materials), excess pore pressures dissipate immediately with Minefill A (aided by the self desiccation mechanism) and the pore pressures in the fill mass are the steady state seepage pore pressures resulting from the reduced flow area in the drawpoint. This steady state seepage is expected to be the prime source of pore pressure in coarse grained fills.

MINEFILL B

For Minefill B, the initial low stiffness and hydraulic conductivity result in very little conventional drainage-type consolidation. Close inspection of Figure 7 indicates that during the early stages of filling, pore pressures in Minefill B are higher than in Minefill A. This is reflected in higher barricade loads during this period. However, this material has a higher propensity for self desiccation, and therefore, after "initial set," the self desiccation mechanism reduces the water volume. This water volume reduction, combined with the increased material stiffness, acts to create a drop in pore pressure after "initial set." For higher permeability materials, this would be counteracted by steady state seepage (as shown for Material A), but for Minefill B, the permeability is low enough that pore pressures are reduced well below the steady state line by the self desiccation mechanism.

Thus, pore pressures below the steady state line may be produced by self desiccation in association with low hydraulic conductivity. To further demonstrate this point, modelling was undertaken using Minefill B material properties but with the hydraulic conductivity increased by an order of magnitude. Intuitively it might be expected that an increase in hydraulic conductivity would result in lower pore pressures. However, the opposite is the case, as can be seen in Figure 9, which shows the development of pore pressure against time for the modified Minefill B material as well as that for the original Minefill B case.

Figure 9 indicates that the increase in hydraulic conductivity has allowed the steady state seepage pore pressures to be restored, increasing pore pressures relative to the low values that were generated as a result of self desiccation in the original case.

The significance of this pore pressure change on barricade loads has been demonstrated in Figure 10, which shows the variation in barricade stresses against time during filling. For comparison purposes, the original Minefill B barricade stresses are also

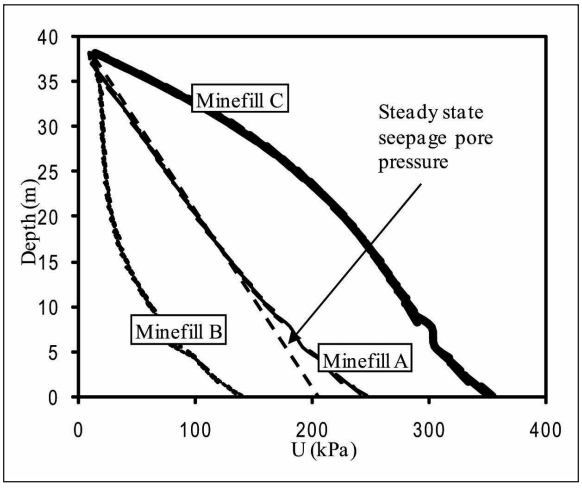

Fig. 8. Pore pressure isochrones.

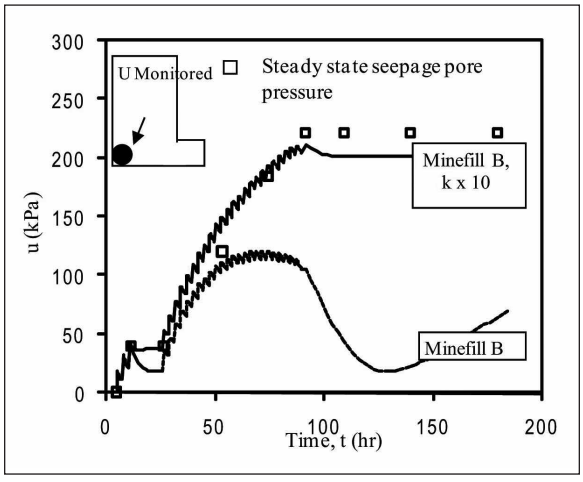

Fig. 9. Development pore pressure with time for Minefill B with increased hydraulic conductivity.

included in Figure 10. For this case, the increase in the hydraulic conductivity has resulted in an increase of about 50% in barricade loads.

It is interesting to note that the pore pressure development and resulting barricade stresses with the modified Minefill B material (increased hydraulic conductivity) are similar to those for the Minefill A case.

The dependence of low pore pressures on both self desiccation and hydraulic conductivity should be considered in the case where tailings are classified to create a coarse paste, or where coarse product is blended with tailings to generate a paste backfill.

MINEFILL C

Like Minefill B, the coefficient of consolidation (i.e. low permeability and high stiffness) of Minefill C is very low, and therefore drainage-induced consolidation is insufficient to dissipate excess pore pressures. However, unlike Minefill B, the propensity for self desiccation is too low to give significant pore pressure reduction, with the result that significant pore pressures develop. These pore pressures are reflected in the high barricade loads that are created.

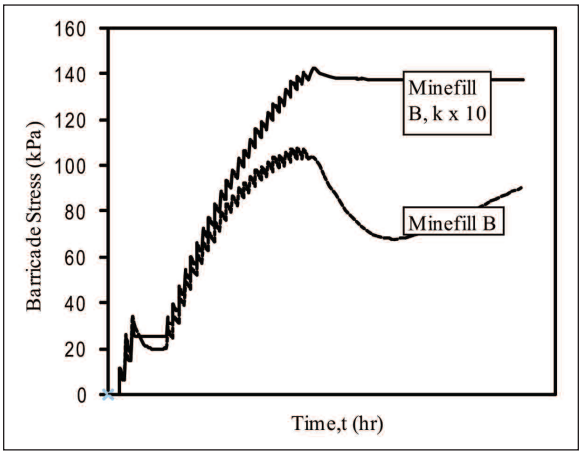

Fig. 10. Barricade load plotted against time for Minefill B with increased hydraulic conductivity, compared to original case.

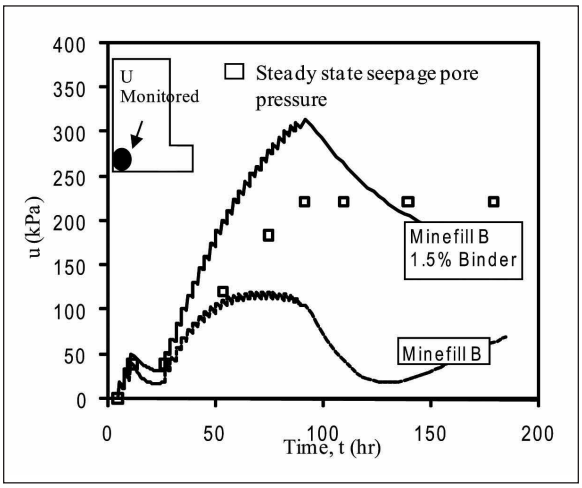

Fig. 11. Pore pressure against time for Minefill B with 1.5% cement content.

This situation may occur when the tailings being used to form the paste have a high clay content. Clay particles will reduce the coefficient of consolidation (suppressing conventional consolidation) and have also been shown to adversely affect the cement hydration process. This is the case with Minefill C.

In addition, where consolidation is dependent on self desiccation, a reduction in binder content can also create this high pore pressure condition through reduced cement concentration (which reduces total self desiccation volume changes) and reduced stiffness.

A numerical experiment has been presented to illustrate the significance of binder content on consolidation. In this example, Minefill B has been simulated but in this case a cement content of 1.5% has been used rather than the original 3%.

Figure 11 shows the development of pore pressure against time for Minefill B with 1.5% cement content. For comparison purposes, the steady state seepage pore pressures and the original Minefill B pore pressures are reproduced in Figure 11. This shows that the reduction in binder content has created a significant increase in the pore pressures that develop within the stope.

The increase in pore pressure associated with the binder reduction leads to a significant increase in barricade loads. This is illustrated in Figure 12, which presents the calculated barricade loads against time for the Minefill B 1.5% cement case compared to the original (3% cement) case. It can be seen that the reduction in binder content from 3% to 1.5% has resulted in a 100% increase in barricade loads.

CONCLUSION

This paper has demonstrated that barricade loads are highly dependent on the degree of consolidation that occurs during filling. As a result, barricade loads cannot be determined solely on the basis of simple strength parameters (e.g. unconfined compression

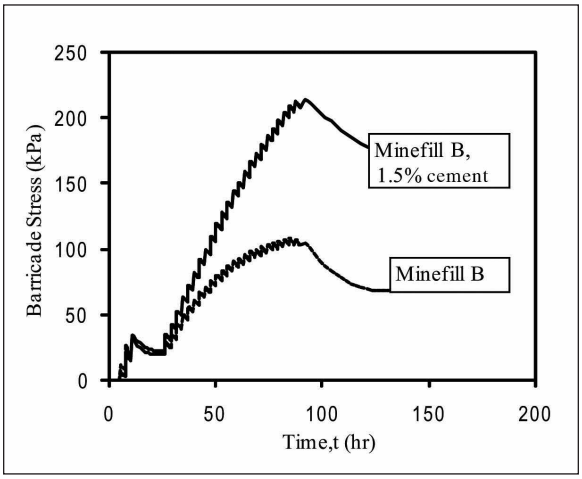

Fig. 12. Barricade load against time for Minefill B with 1.5% cement content.

strength q_u). Rather, subtle variations in material properties such as hydraulic conductivity and the chemical reactions associated with the binder reactions can have a significant influence on barricade loads.

The work has also demonstrated that rather than any individual material property dominating the behaviour, the response during filling is the result of interaction between a number of different material properties. In general, these interactions are complex, and hence fully coupled methods of analysis, such as the one incorporated in Minefill 2-D, are required to predict the behaviour.

An interesting example of this interaction has been presented showing that (contrary to conventional consolidation theory) an increase in material hydraulic conductivity can actually act to increase pore pressures and hence increase barricade stresses. When combined with a high propensity for self desiccation, low permeability can actually result in low pore pressures during and for some time following hydration.

The overall message that the authors have attempted to convey in this work is that adopting simple "rules of thumb" for paste or hydraulic fills can be dangerous, and care should be exercised when developing new backfill systems or modifying mix designs, as these modifications may completely change the overall barricade loading mechanism.

ACKNOWLEDGMENTS

The authors would like to acknowledge the support of the UWA Gledden Postgraduate Scholarships Foundation, the Shaw Memorial Postgraduate Scholarship Foundation, and MERIWA (the Minerals and Energy Research Institute of Western Australia) for their financial contribution to this research.

Paper reviewed and approved for publication by the Minefill 2007 Symposium review committee.

Matt Helinski has a Bachelor's degree in civil engineering from the University of Newcastle. After working as a geotechnical engineer in the civil and mining industries for six years, Matt commenced PhD studies in the field of mine backfill geomechanics. Matt is currently in the process of completing his PhD and also works as a consultant with Revell Resources, a small group that specializes in mine backfill consulting.

Martin Fahey has degrees in mathematics and engineering science (Trinity College, Dublin, 1976) and a PhD in soil mechanics (Cambridge University, 1980). He joined the geotechnical consulting company Golder Associates in 1981, and then the School of Civil and Resource Engineering at The University of Western Australia in 1984, where he is currently a professor of civil engineering. He is a founding director of the geotechnical consulting company Advanced Geomechanics.

Andy Fourie has Bachelor's and Master's degrees in engineering from the University of the Witwatersrand (Wits). After working for geotechnical consulting company SRK Consulting, he obtained a PhD in geotechnical engineering from Imperial College, London. He was a Lecturer at the University of Queensland before moving to Wits, becoming a professor of civil engineering. He is currently Principal at the Australian Centre for Geomechanics, with research and training activities in mine waste management and mine closure.

REFERENCES

Baig, S., Picornell, M., & Nazarian, S. (1997). Low strain shear moduli of cemented sands. *Journal of Geotechnical and Geoenvironmental Engineering, ASCE*, *123*, 540-545.

Belem, T., El Aatar, O., Bussière, B., Benzaazoua, M., Fall, M., & Yilmaz, E. (2006). Characterization of self-weight consolidated paste backfill. In R. Jewell, S. Lawson, & P. Newman (Eds.), *Paste 2006: Proceedings of the 9th International Seminar on Paste and Thickened Tailings* (pp. 333-345). Perth: Australian Center for Geomechanics, University of Western Australia.

Biot, M.A. (1941). General theory of three dimensional consolidation. *Journal of Applied Physics*, *12*, 154-164.

Carrier, W.D., Bromwell, L.G., & Somogyi, F. (1983). Design capacity of slurried mineral waste ponds. *Journal Geotechnical Engineering Division, ASCE*, *109*, 699-716.

Dyvik, R., & Olsen, T.S. (1989). G_{max} measured in oedometer and DSS tests using bender elements.. *Proceedings of the 12th International Conference on SMFE* (pp. 39-42). Rio de Janeiro: Balkema.

Fahey, M., & Carter, J.P. (1993). A finite element study of the pressuremeter test in sand using a non-linear elastic plastic model. *Canadian Geotechnical Journal*, *30*, 348–362.

Fernandez, A., & Santamarina, J.C. (2001). Effect of cementation on the small strain parameters of sand. *Canadian Geotechnical Journal*, *38*, 191-199.

Helinski, M., Fourie, A.B., & Fahey, M. (2006). Mechanics of early age cemented paste backfill. In R. Jewell, S. Lawson, & P. Newman (Eds.). *Paste 2006—Proceedings of the 9th International Seminar on Paste and Thickened Tailings* (pp. 313-322). Perth: Australian Centre for Geomechanics, University of Western Australia.

Helinski, M., Fourie, A.B., & Fahey, M. (2007). The self desiccation process in cemented mine backfill. *Canadian Geotechnical Journal* (*in press*).

Helinski, M., & Grice, A.G. (2007). Water management in hydraulic fill operations. In J. Archibald, & F. Hassani (Eds.). *Minefill '07* (Paper #2481). Montreal: CIM.

Isaacs, L.T., & Carter, J.P. (1993). Theoretical study of pore pressure developed in hydraulic fill in mine stopes. *Transactions of the Institution of Minerals and Metallurgy*, *92*, A93-A102.

Le Roux, K.A., Bawden, W.F., & Grabinski, M.W.F (2002). Assessing the interaction between hydration rate and fill rate for a cemented paste backfill. *Proceedings of the 55th Canadian Geotechnical and 3rd joint IAH-CNC groundwater specialty conference* (pp. 427-432). Niagara Falls: Cédérom.

Rankine, R.M., Rankine, K.J., Sivakugan, N., Karunasena, W., & Bloss, M. (2001). A numerical analysis of the arching mechanism in pastefill throughout a complete mining sequence. In S. Valliapan & N. Khalili (Eds.). *Proceedings of the First Asian Pacific Congress on Computational Mechanics* (pp. 461-466). Sydney: Elsevier.

Rastrup, E. (1956). The temperature function for heat of hydration in concrete, RILEM Symposium on Winter Concreting, Copenhagen: Danish Institute for Building Research.

Revell, M.B. (2004). Paste—How strong is it? *Proceedings of the 8th International Symposium on Mining with Backfill* (pp. 286-294). Beijing: The Nonferrous Metals Society of China.

Traves, W.H., & Isaacs, L.T. (1991). Three-dimensional modelling of fill drainage in mine stopes. *Transactions of the Institution of Minerals and Metallurgy*, (Section A: Min. Industry), *100,* A66-A72.

  ISSN 1718-4169